Journal of Nuclear Medicine, published on November 2, 2018 as doi:10.2967/jnumed.118.219097

Principal component analysis of brain metabolism predicts development of Alzheimer's dementia

Ganna Blazhenets[1], Yilong Ma[2], Arnd Sörensen[1], Gerta Rücker[3], Florian Schiller[1], David Eidelberg[2], Lars Frings[1,4] and Philipp T. Meyer[1] for the Alzheimer's Disease Neuroimaging Initiative*[a]

Short running title: **AD conversion-related metabolic network**

[1]Department of Nuclear Medicine, Medical Center – University of Freiburg, Faculty of Medicine, University of Freiburg, Freiburg, Germany

[2]Center for Neurosciences, The Feinstein Institute for Medical Research, Manhasset, NY, USA

[3]Institute of Medical Biometry and Statistics, Medical Center – University of Freiburg, Faculty of Medicine, University of Freiburg, Freiburg, Germany

[4]Center for Geriatrics and Gerontology Freiburg, Medical Center - University of Freiburg, Faculty of Medicine, University of Freiburg, Freiburg, Germany

Word count: 5179

Corresponding Author: G. Blazhenets, Hugstetter Str. 55, 79106, Freiburg, Germany.

ganna.blazhenets@uniklinik-freiburg.de, Tel: +0049 761 270 38861.

* Data used in preparation of this article were obtained from the Alzheimer's Disease Neuroimaging Initiative database (adni.loni.usc.edu). As such, the investigators within the ADNI contributed to the design and implementation of ADNI and/or provided data but did not participate in analysis or writing of this report.

ABSTRACT

The predictive value of 18F-fluorodeoxyglucose (FDG) PET for conversion from mild cognitive impairment (MCI) to Alzheimer's dementia (AD) is currently under debate. We used a principal component analysis (PCA) to identify a metabolic AD conversion-related pattern (ADCRP) and investigated the prognostic value of the resulting pattern expression score (PES).

Methods: FDG PET scans of 544 MCI patients obtained from the Alzheimer's Disease Neuroimaging Initiative (ADNI) database were analyzed. We implemented voxel-based PCA and standard SPM (as reference) analyses to disclose cerebral metabolic patterns associated with conversion from MCI to AD. By Cox proportional hazards regression we examined the prognostic value of candidate predictors. Also, we constructed prognostic models with: i) clinical, ii) imaging, and iii) clinical and imaging variables in combination.

Results: PCA revealed an ADCRP that involved regions with relative decrease in metabolism (temporoparietal, frontal, posterior cingulate and precuneus cortex) and relative increase in metabolism (sensorimotor and occipital cortex, cerebellum and left putamen). Among the predictor variables age, sex, functional activities questionnaire (FAQ), mini-mental state examination (MMSE), apolipoprotein E (APOE), PES and normalized FDG uptake (regions with significant hypo- and hypermetabolism in converters compared to non-converters), PES was the best independent predictor of conversion (Hazard Ratio = 1.77 per z-score increase, 95% C.I.: 1.24 - 2.52, $p < 0.001$). Moreover, adding PES to the model including the clinical variables significantly increased its prognostic value.

Conclusions: The ADCRP expression score is a valid predictor of conversion. Combining clinical variables and PES yielded a higher accuracy than each single tool in predicting conversion of MCI to AD, underlining the incremental utility of FDG PET.

Keywords: Alzheimer's dementia, Mild cognitive impairment, PCA, Cox model, FDG PET.

INTRODUCTION

Subjects with mild cognitive impairment (MCI) are at high risk of converting to Alzheimer's dementia (AD), but they can also develop a different type of dementia, remain stable or even regress to a normal aging process (*1*). Various studies have shown that MCI patients exhibit metabolic changes that can be detected with ^{18}F-fluorodeoxyglucose (FDG) PET (*2-5*). However, a limited prediction accuracy of conversion from MCI to AD by FDG PET was reported by some studies (*6-8*). Likewise, a Cochrane review did not recommend using FDG PET for this purpose (*9*), although this has been a matter of controversy (*10*).

Principal component analysis (PCA) was proposed as an alternative voxel-wise approach of image analysis for the diagnosis of neurodegenerative disorders. PCA has shown its value in the development of disease-specific spatial covariance patterns of regional metabolism characterizing disorders like Parkinson's disease (PD), multiple system atrophy, progressive supranuclear palsy, and corticobasal degeneration (*11-15*). Moreover, a high predictive value of PCA was shown in PD with cognitive decline, suggesting that the pattern expression score (PES) of a PD-cognition related pattern is a useful biomarker for prediction of conversion of PD-MCI to PD with dementia (*16,17*). In this study, we used PCA and FDG PET to determine whether there is a specific metabolic pattern associated with conversion of MCI to AD (termed AD conversion-related pattern, ADCRP). In particular, we aimed to examine the potential of ADCRP expression alone and in combination with clinical variables for predicting the conversion of MCI to AD.

MATERIALS AND METHODS

Patients' Data and Diagnoses

FDG PET scans obtained from the Alzheimer's Disease Neuroimaging Initiative (ADNI, ClinicalTrials.gov Identifier: NCT00106899) were used in this study. The ADNI was launched in 2003 as a public-private partnership, led by Principal Investigator Michael W. Weiner, MD. The information about study protocols and ADNI project can be found at www.adni-info.org. The study was approved by ADNI and written informed consent was obtained by ADNI from all subjects and before protocol-specific procedures are carried out (see ADNI protocols).

For the present analysis we used ADNI 1, ADNI 2 and ADNI GO cohorts. Participants (n = 576) were evaluated at baseline, and in 6 to 12-month intervals following initial evaluation for up to 10 years. FDG-PET scans acquired at the baseline visit were used in the present analysis. We included the subjects who were diagnosed with MCI and had a mini-mental state examination (MMSE) score of at least 24 points at the time of PET imaging (n = 6 excluded). Additionally, we requested a minimal follow-up time of at least 6 months (n = 20 excluded, among them n = 10 without follow-up). Furthermore, subjects with a bidirectional change of diagnosis (MCI to AD, and back to MCI) within the follow-up time were excluded (n = 6). The remaining 544 subjects were dichotomized into MCI patients who converted to AD (MCI converters, MCI-c) and those who did not (MCI non-converters, MCI-nc).

The data was randomly split into training and test datasets of equal sizes (n = 272). Age, sex, MMSE and median follow-up time did not differ significantly among two datasets ($p > 0.1$). As expected, the rate of apolipoprotein E (APOE) ε4 carriers was significantly higher and functional activities questionnaire (FAQ) was significantly lower for MCI-c versus MCI-nc in

each of the datasets but comparable per subgroup between the two datasets. The clinical and demographic characteristics of the datasets are given in Table 1.

PET Imaging

The PET data acquisition details can be found online in the study protocols of the ADNI project. In 487 cases dynamic 3D scans with six 5-min frames were acquired 30 minutes after injection of 185 ± 18.5 MBq FDG. In the rest of the cases (N = 57), patients were scanned with a static 30-minutes acquisition. In case of dynamic scans, all frames were motion-corrected to the first frame and then summed up to create a single image file.

Individual scans were spatially normalized onto an in-house FDG PET template in Montreal Neurological Institute brain space and smoothed with an isotropic Gaussian kernel of 12 mm full-width at half maximum. All preprocessing was implemented with an in-house pipeline in MATLAB (The MathWorks, Inc., Natick, Massachusetts, United States) and Statistical Parametric Mapping (SPM12) software (www.fil.ion.ac.uk/spm) following recommendations for optimal statistical analysis of brain FDG PET scans in the context of MCI to AD conversion (*18*).

Multivariate Principal Component Analysis

Scaled subprofile model (SSM) PCA was used to generate an SSM pattern based on group discrimination between MCI-c and MCI-nc. It was implemented on the training dataset of 272 subjects using the Scanvp/SSMPCA toolbox (*19*). Each subject's 3D image data was first converted to a continuous row vector, and then embedded in a group data matrix. Each data entry was transformed to logarithmic form, and data matrix was centered by each row mean value. The

deviation from both subject and group means represents the resulting subject residual profile image. PCA is applied to the covariance matrix to derive orthogonal eigenvectors and associated eigenvalues. These spatial eigenvectors are principal components (PC) image patterns given by the SSM/PCA analysis.

PCs related to the explored group difference are associated with the highest total variance accounted for by the eigenvector. To delineate topographies associated with conversion from MCI to AD, we performed voxel-wise PCA on the combined group of MCI-c and MCI-nc in the training dataset. To identify a significant pattern, different combinations of PCs were tested based upon the following statistical criteria: the analysis was limited to the first set of contiguous PCs that account for the top 50% of the variability in the dataset, and the best combination of these PCs was selected by a logistic regression analysis with group (i.e., MCI-c and MCI-nc) as the dependent variable and subject scores for the PCs as the independent variable. The obtained ADCRP represents spatially covariant voxels associated with the conversion to AD, with each voxel being specifically weighted towards its relative contribution. For both, training and test datasets each individual's PES of the ADCRP was evaluated by the topographical profile rating algorithm involving computation of the internal vector product of the subject's residual profile vector and the pattern vector (*20*).

Additionally, we performed a voxel-wise two-sample t-test between FDG scans of MCI-c and MCI-nc from the training dataset by SPM. This analysis compared differences in normalized FDG uptake by applying proportional scaling to minimize the effect of inter-subject variability of global FDG uptake. The p-value adjustment for contrasts was set to family-wise error corrected (FWEC) $p < 0.05$. The resulting volumes of interest (SPM VOIs) comprising all significant clusters of relative hypo- and hypermetabolism were then used to extract the

individual normalized FDG uptake inside these SPM VOIs after the subject's scan has been normalized using a predefined mask of brain parenchyma. Mean uptake in the hypo- and hypermetabolic VOIs were linearly combined with weighting defined by logistic regression. Mean uptake in only hypometabolic clusters was also included for comparison given that this is a commonly used measure of abnormal brain regions in clinical dementia imaging.

Cox Model Analysis

For each individual the baseline time was considered to be the time of the PET imaging, and the end point was chosen to be the time of AD diagnosis for MCI-c or last follow-up time for MCI-nc. Cox proportional hazards regression models were calculated in R (http://www.R-project.org/) employing the 'Survival' package (*21*) in order to test the predictive value of the following FDG PET variables and clinical variables for conversion from MCI to AD: PES (ADCRP from PCA), mean normalized FDG uptake (within SPM VOIs), FAQ, APOE ε4 genotype (positive or negative for the presence of at least one ε4 allele), and MMSE. Cox model analyses were adjusted for age at baseline (years) and sex (1 for male, 0 for female). All continuous covariates were z-transformed such that the hazard ratio (HR) reflects risk changes per standard deviation increase.

First, in order to compare the HR of independent predictor variables, a Cox model including all predictors (PES, normalized FDG uptake, FAQ, APOE, MMSE, age and sex) was computed on the training dataset using the ridge regression option to account for multicollinearity.

Second, we examined three Cox models including identified significant predictors adjusted for age and sex for the training dataset with: i) clinical (FAQ, APOE and MMSE), ii)

imaging (PES of ADCRP), and iii) combined (FAQ, APOE, MMSE and PES) variables. The prediction accuracy of each model was statistically compared by Harrell's concordance C.

For the sake of validation of the constructed models, the results of each Cox model were independently applied to the test dataset via calculation of the prognostic index (PI) for each subject (*22*). Here, the PI is the sum of the product of the regression coefficients β_i and predictor variables x_i (with i being the index for the order of predictors in the model), as follows: $\mathrm{PI} = \beta_1 x_1 + \cdots + \beta_i x_i$. Based on the values of PI, the test dataset was stratified into three equally-sized risk groups. Separation between models was compared by Kaplan-Meier survival curves and Akaike information criterion (AIC). Risk group separation based on PI values of the combined model (FAQ, APOE, MMSE and PES) was compared to group separation based on PES values only (i.e., 'raw' values of PES, not PI).

RESULTS

AD Conversion-Related Pattern

We limited the PCs estimated by our SSM/PCA analysis to the first seven PCs that accounted for 52.05% of the total variance. However, only PCs number 2, 3, 6, and 7 were selected by logistic regression and showed a significant between-group difference after Bonferroni correction ($p < 0.05$). The logistic regression model including these PCs yielded the highest significance and lowest AIC in comparison to the other combinations. Therefore, PC2, PC3, PC6 and PC7 were linearly combined to yield the ADCRP (Figure 1A), which allows for a significant separation between groups of MCI-c and MCI-nc ($p = 9\times10^{-13}$). For comparison, the more restricted, although overlapping pattern of regions with significant hypo- and hypermetabolism in MCI-c compared to MCI-nc derived by SPM is shown in Figure 1B.

The most prominent decreases of metabolism in MCI-c compared to MCI-nc on ADCPR were found in the temporoparietal cortex as well as the precuneus/posterior cingulate cortex. Furthermore, decreases were also found in the right frontal cortex, but with a lower factor loading to the pattern in total. Relative increases (probably corresponding to regions with preserved metabolic activity) were detected in sensorimotor and occipital cortices, cerebellum, and in the left putamen.

Topographical profile rating of ADCRP for each subject of the training and test datasets resulted in a PES, which can be used to assess the degree to which a subject expresses this pattern. There was no difference in PES between the two MCI-c groups (training vs test dataset, $p > 0.1$) or between the two MCI-nc groups (training vs test dataset, $p > 0.1$). Based on receiver operating characteristics (ROC) analyses, the area under ROC curve (AUC) for separation between MCI-c and MCI-nc reached AUC = 0.749 in the training dataset and AUC = 0.761 in

the test dataset, which verifies high stability of the pattern across the subject cohorts. Similar separation was achieved based on mean normalized FDG uptake values obtained with the linear combination in both hyper- and hypometabolic SPM VOIs (normalized FDG uptake = -4.82 + 12.52 * mean FDG uptake in hypometabolic clusters - 9.52 * mean FDG uptake in hypermetabolic clusters): AUC = 0.758 for the training dataset and AUC = 0.760 for the test dataset. Normalized FDG uptake in the hypometabolic VOI alone showed a lower AUC, but was included for comparison as a commonly used measure of abnormal brain regions (Supplementary Figure 1).

Cox Models

First, in the training dataset the Cox proportional hazards regression with age, sex, FAQ, MMSE, APOE, PES and normalized FDG uptake as predictors was computed, penalized by ridge regression to suppress collinearity among predictors (Figure 2). PES (ADCRP), normalized FDG uptake (SPM VOIs), FAQ and MMSE were significant predictors, with PES having the highest HR of 1.77 (95% C.I.: 1.24 - 2.52, $p < 0.001$).

Then, we examined (1) imaging and (2) clinical models, and later joined them into (3) a combined Cox model to investigate a possible additive prognostic value of PES to the clinically established predictors APOE, FAQ and MMSE. The variables included in each model and their corresponding HRs are presented in Table 2. The results of the imaging Cox model showed PES to be a significant predictor for conversion from MCI to AD with the hazard ratio for z-transformed PES of 2.96 (95% C.I.: 2.35 - 3.74, $p = 2\times10^{-16}$). Age and sex were no significant predictors in any of the models.

While the clinical model (Harrell's C = 0.80) showed higher accuracy than the imaging model (Harrell's C = 0.76), adding PES to the clinical variables significantly ($p < 0.001$) increased the prognostic value (combined clinical variables and PES: Harrell's C = 0.84). The quality of statistical models was tested with the AIC test (combined model AIC = 749.6, imaging model AIC = 783.3, clinical model AIC = 797.2): the combined model was significantly better than the imaging model ($p < 0.001$), and the imaging model significantly better than the clinical model ($p = 0.007$). Thus, the combined model is the preferred model with the minimum AIC value.

Second, Cox models were validated on the test dataset. We obtained PIs that were used for the survival analysis. Similar to the training dataset, the clinical model of the test dataset had a higher Harrell's C than the imaging model (C = 0.77 vs. C = 0.73, respectively). The increase of the prognostic value of the clinical model, when PES was added as a predictor to yield the combined model, was also confirmed in the test dataset (combined model C = 0.81).

Normalized FDG uptake (SPM VOIs) as a single predictor showed a lower HR and significance level compared to PES (ADCRP), see Figure 2. However, as it is a commonly used measure in neuroimaging analysis, we constructed similar clinical, imaging and combined Cox models with normalized FDG uptake (analogously to those with PES): significant increase in predictive value of the clinical model (C = 0.80 and C = 0.77, for the training and test datasets respectively) was observed when FDG uptake was added as predictor (imaging model C = 0.76 and C = 0.73; combined model C = 0.84 and C = 0.81), and AIC indicated the combined model as the best model.

The combined model with normalized FDG uptake (SPM VOIs) had a significantly lower predictive value than the combined model with PES (combined model with PES: AIC = 749.6,

combined model with normalized FDG uptake: AIC = 751.6; $p < 0.001$, likelihood-ratio test). The detailed results of the clinical, imaging and combined Cox models with normalized FDG uptake for the training and test datasets can be found in supplementary materials (Supplementary Table 1).

Risk Group Stratification

In the test dataset, we tested whether risk groups were better separated by PI derived from the combined model (including PES) or by PES values alone (Figure 3). Both models demonstrated a good separation between three groups with high, medium and low risk of conversion to AD. The best stratification was reached with the PI resulting from the combined model. This method allows accounting for all available variables at once including time to conversion of the training dataset used for definition of the Cox model. The most noticeable difference is observed in the first 60 months and comparison between the risk strata is statistically limited after this time point due to the small number of subjects left (Table 3).

DISCUSSION

Using FDG PET data in a combination with voxel-based PCA we identified a metabolic pattern associated with conversion from MCI to AD. Aside from constructing the ADCRP, we estimated its predictive accuracy in a large cohort of subjects and prospectively confirmed its validity on the test dataset.

The obtained network topography is consistent with previously published hypo- and hypermetabolic regions identified in AD (*3,17,23,24*). We found that conversion to AD is characterized by a significant metabolic decrease in temporoparietal regions, right frontal cortex, posterior cingulate and precuneus cortex, while occipital cortex, sensorimotor cortex, cerebellum, and left putamen showed relatively increased metabolic activity. The latter most likely corresponds to preserved metabolic activity, given that proportional scaling by global uptake was performed. We also analyzed the same groups of subjects with SPM t-test, which indicated overlapping regions of hypo- and hypermetabolism, which, however, were much more restricted.

Although we observed some similarities between the topography of ADCRP and the distribution of regional metabolic differences depicted by SPM in the current study, these results portray very different measures of brain function. Indeed, the ADCRP from spatial covariance analysis uses variance information of glucose metabolism measured on FDG PET. By contrast, maps of SPM t-test revealed regional differences in mean value of normalized glucose metabolism. It has been shown consistently that the PCA approach has a higher sensitivity compared to SPM group comparisons regarding the detection of brain regions with metabolic changes in neurodegenerative disorders such as AD (*23*) and PD (*25*), or in subjects with idiopathic rapid eye movement sleep behavior disorder (*26,27*). This is further supported by the

observation that the pattern expression score of the AD-related pattern (ADRP) had a higher accuracy in group discrimination than metabolic changes measured in regions of interest (*23,28*). Superior performance of PES as a predictor compared to normalized uptake in SPM VOIs in the present study is consistent with these prior results. Moreover, the computation of the degree of pattern expression in the individual patient is performed automatically and blind to the clinical information. Thus, this approach is potentially more objective than any diagnostic categorization achieved by visual reads or predefined ROI analysis.

In contrast to the ADRP of Teune et al. (*24*), we focused our study not on the differences between AD and normal elderly controls, but on the prodromal phase of AD. The metabolic pattern at the MCI stage might be particularly influenced by compensatory neural mechanisms (*29*), which may be reflected in the metabolic pattern. However, Meles et al. (*30*) investigated the expression of the ADRP (*24*) in an MCI cohort and reported a comparable AUC (AUC = 0.80). Similarly to the papers mentioned above, we observed a significant inverse correlation between PES and MMSE ($r = -0.27$, $p < 0.001$). In addition, we found significant positive correlation between PES and clinical dementia rating scale sum of the boxes ($r = 0.37$, $p < 0.001$), and PES and Alzheimer's disease assessment scale (cognitive subscale total 11 sum score) ($r = 0.36$, $p < 0.001$), indicating a significant association between expression of the detected pattern and cognitive impairment. No correlation was found for PES and sex or age in both datasets (not shown in detail).

Although various biomarkers have been already examined as predictors in regression models, our study examined imaging (PES; normalized FDG uptake in linearly combined VOIs with significant hypo- and hypermetabolism) along with genetic (APOE), sociodemographic (age, sex), and cognitive (FAQ, MMSE) variables in Cox model analyses to rate the progression

of MCI to AD. As a single predictor, PES has shown a higher hazard ratio than FAQ, MMSE, APOE or normalized FDG uptake. We found that the imaging Cox model with PES was comprehensive, and provided significant enhancement in predicting conversion when combined with clinical variables. Since ROC analysis does not include time-to-event information, the AIC and Harrell's C were used instead to evaluate the performance of the prediction. The combination of imaging and clinical variables gave the best prediction similarly to the study by Liu et al. (*3*).

It was shown that PES could be applied to a new subject on a single-case basis, despite the subjects have been scanned on different PET systems (*12,30*). The benefit of the current study is the ability to combine the disease-related network pattern with the clinical variables to obtain per subject a quantifiable prognostic index for the conversion of MCI to AD. While PES itself is a good predictor and can be used to predict conversion, the combination of PES with clinical variables and calculation of PI gives better stratification, which may be a particularly attractive approach for single-subject predictions (Figure 3). For instance, a subject might be assigned to one of the defined groups based on its PI value, and acquainted with its most probable median 'conversion-free' time. These results are of great importance not only from a research standpoint (e.g., patient involvement in clinical trials) but also for clinical purposes.

CONCLUSION

Our results confirm the predictive value of FDG PET in patients with MCI. The PCA technique showed its applicability for the differentiation between MCI subjects converting to AD and stable MCI subjects. The PES of the ADCRP was identified as a valid predictor of conversion, and the combination of clinical variables with PES yielded a higher predictive value than each single tool.

DISCLOSURE

The authors declare they did not receive any funding for this study and have no conflict of interest.

REFERENCES

1. Petersen RC, Parisi JE, Dickson DW, et al. Neuropathologic features of amnestic mild cognitive impairment. *Arch Neurol.* 2006;63:665-672.

2. Caroli A, Prestia A, Chen K, et al. Summary metrics to assess Alzheimer disease-related hypometabolic pattern with 18F-FDG PET: head-to-head comparison. *J Nucl Med.* 2012;53:592-600.

3. Liu K, Chen K, Yao L, Guo X. Prediction of mild cognitive impairment conversion using a combination of independent component analysis and the cox model. *Front Hum Neurosci.* 2017;11:33.

4. Nobili F, Salmaso D, Morbelli S, et al. Principal component analysis of FDG PET in amnestic MCI. *Eur J Nucl Med Mol Imaging.* 2008;35:2191-2202.

5. Pagani M, Nobili F, Morbelli S, et al. Early identification of MCI converting to AD: a FDG PET study. *Eur J Nucl Med Mol Imaging.* 2017;44:2042-2052.

6. Frings L, Hellwig S, Bormann T, Spehl TS, Buchert R, Meyer PT. Amyloid load but not regional glucose metabolism predicts conversion to Alzheimer's dementia in a memory clinic population. *Eur J Nucl Med Mol Imaging.* 2018;45(8):1442-1448.

7. Grimmer T, Wutz C, Alexopoulos P, et al. Visual versus fully automated analyses of 18F-FDG and amyloid PET for prediction of dementia due to Alzheimer disease in mild cognitive impairment. *J Nucl Med.* 2016;57:204-207.

8. Trzepacz PT, Yu P, Sun J, et al. Comparison of neuroimaging modalities for the prediction of conversion from mild cognitive impairment to Alzheimer's dementia. *Neurobiol Aging.* 2014;35:143-151.

9. Smailagic N, Vacante M, Hyde C, Martin S, Ukoumunne O, Sachpekidis C. (1)(8)F-FDG PET for the early diagnosis of Alzheimer's disease dementia and other dementias in people with mild cognitive impairment (MCI). *Cochrane Database Syst Rev.* 2015;1:Cd010632.

10. Morbelli S, Garibotto V, Van De Giessen E, et al. A Cochrane review on brain [(1)(8)F]FDG PET in dementia: limitations and future perspectives. *Eur J Nucl Med Mol Imaging.* 2015;42:1487-1491.

11. Eckert T, Tang C, Ma Y, et al. Abnormal metabolic networks in atypical parkinsonism. *Mov Disord.* 2008;23:727-733.

12. Tang CC, Poston KL, Eckert T, et al. Differential diagnosis of parkinsonism: a metabolic imaging study using pattern analysis. *Lancet Neurol.* 2010;9:149-158.

13. Ma Y, Tang C, Spetsieris PG, Dhawan V, Eidelberg D. Abnormal metabolic network activity in Parkinson's disease: test-retest reproducibility. *J Cereb Blood Flow Metab.* 2007;27:597-605.

14. Niethammer M, Tang CC, Feigin A, et al. A disease-specific metabolic brain network associated with corticobasal degeneration. *Brain.* 2014;137:3036-3046.

15. Meyer PT, Frings L, Rucker G, Hellwig S. (18)F-FDG PET in Parkinsonism: differential diagnosis and evaluation of cognitive impairment. *J Nucl Med.* 2017;58:1888-1898.

16. Huang C, Mattis P, Perrine K, Brown N, Dhawan V, Eidelberg D. Metabolic abnormalities associated with mild cognitive impairment in Parkinson disease. *Neurology.* 2008;70:1470-1477.

17. Mattis PJ, Niethammer M, Sako W, et al. Distinct brain networks underlie cognitive dysfunction in Parkinson and Alzheimer diseases. *Neurology.* 2016;87:1925-1933.

18. Lange C, Suppa P, Frings L, Brenner W, Spies L, Buchert R. Optimization of statistical single subject analysis of brain FDG PET for the prognosis of mild cognitive impairment-to-Alzheimer's disease conversion. *J Alzheimers Dis.* 2016;49:945-959.

19. Eidelberg D. Metabolic brain networks in neurodegenerative disorders: a functional imaging approach. *Trends Neurosci.* 2009;32:548-557.

20. Spetsieris PG, Eidelberg D. Scaled subprofile modeling of resting state imaging data in Parkinson's disease: methodological issues. *Neuroimage.* 2011;54:2899-2914.

21. Therneau TM, Grambsch PM. *Modeling Survival Data: Extending the Cox Model*. New York, NY: Springer; 2000:39-77.

22. Royston P, Altman DG. External validation of a Cox prognostic model: principles and methods. *BMC Med Res Methodol.* 2013;13:33.

23. Habeck C, Foster NL, Perneczky R, et al. Multivariate and univariate neuroimaging biomarkers of Alzheimer's disease. *Neuroimage.* 2008;40:1503-1515.

24. Teune LK, Strijkert F, Renken RJ, et al. The Alzheimer's disease-related glucose metabolic brain pattern. *Curr Alzheimer Res.* 2014;11:725-732.

25. Ma Y, Tang C, Moeller JR, Eidelberg D. Abnormal regional brain function in Parkinson's disease: truth or fiction? *Neuroimage.* 2009;45:260-266.

26. Ge J, Wu P, Peng S, et al. Assessing cerebral glucose metabolism in patients with idiopathic rapid eye movement sleep behavior disorder. *J Cereb Blood Flow Metab.* 2015;35:2062-2069.

27. Wu P, Yu H, Peng S, et al. Consistent abnormalities in metabolic network activity in idiopathic rapid eye movement sleep behaviour disorder. *Brain.* 2014;137:3122-3128.

28. Asllani I, Habeck C, Scarmeas N, Borogovac A, Brown TR, Stern Y. Multivariate and univariate analysis of continuous arterial spin labeling perfusion MRI in Alzheimer's disease. *J Cereb Blood Flow Metab.* 2008;28:725-736.

29. Clement F, Belleville S. Effect of disease severity on neural compensation of item and associative recognition in mild cognitive impairment. *J Alzheimers Dis.* 2012;29:109-123.

30. Meles SK, Pagani M, Arnaldi D, et al. The Alzheimer's disease metabolic brain pattern in mild cognitive impairment. *J Cereb Blood Flow Metab.* 2017;37:3643-3648.

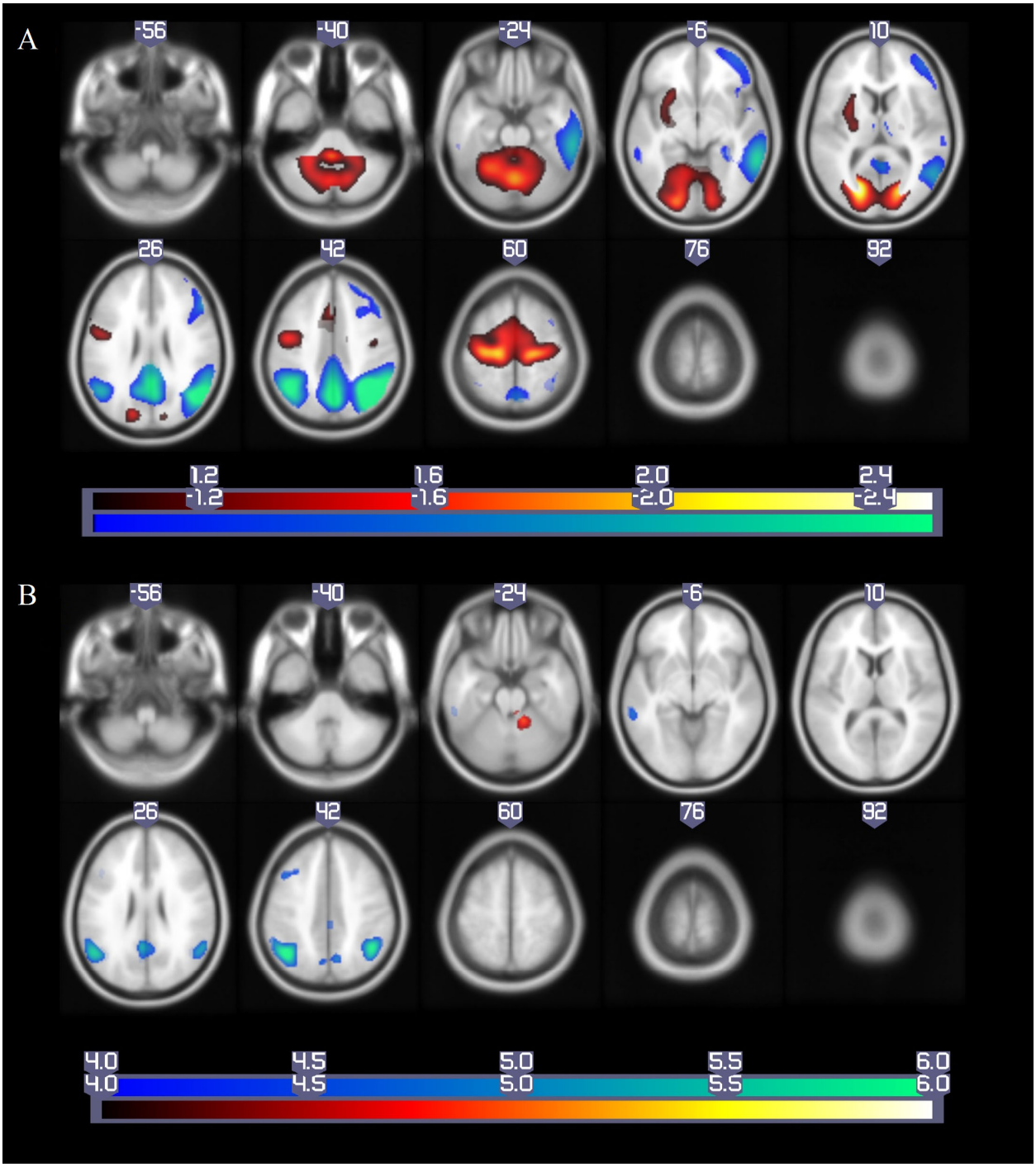

FIGURE 1. Patterns of regional brain metabolism. (A) ADCRP derived by PCA ($p < 0.05$) and (B) significant regions derived by SPM t-test (SPM {T}, FWEC $p < 0.05$), overlaid on MRI template image. Voxels with negative region weights and hypometabolism are given in 'cool' colors, and regions with positive region weights and hypermetabolism are depicted in 'hot'

colors. Data is presented in neurological orientation. ADCRP, Alzheimer's dementia conversion related pattern; PCA, principal component analysis.

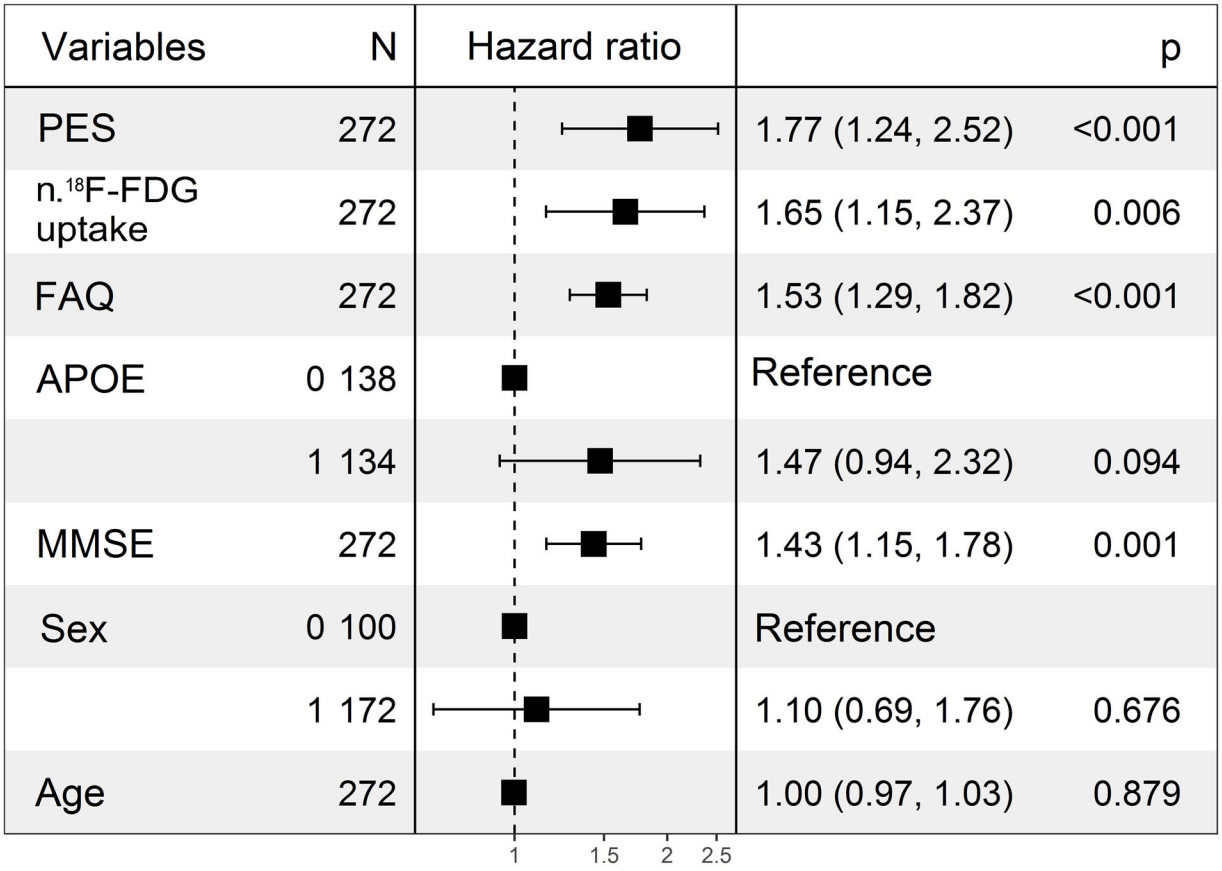

FIGURE 2. Hazard ratios of different predictors, penalized by ridge regression to suppress the effects of multicollinearity among them. Normalized FDG uptake stems from a linear combination of normalized FDG uptake in VOIs with significant hypo- and hypermetabolism. APOE reference: APOE positive, sex reference: female. PES, pattern expression score; n., normalized; FAQ, functional activities questionnaire total score; APOE, apolipoprotein E; MMSE, mini-mental state examination; N, number of subjects. All continuous variables are z-transformed.

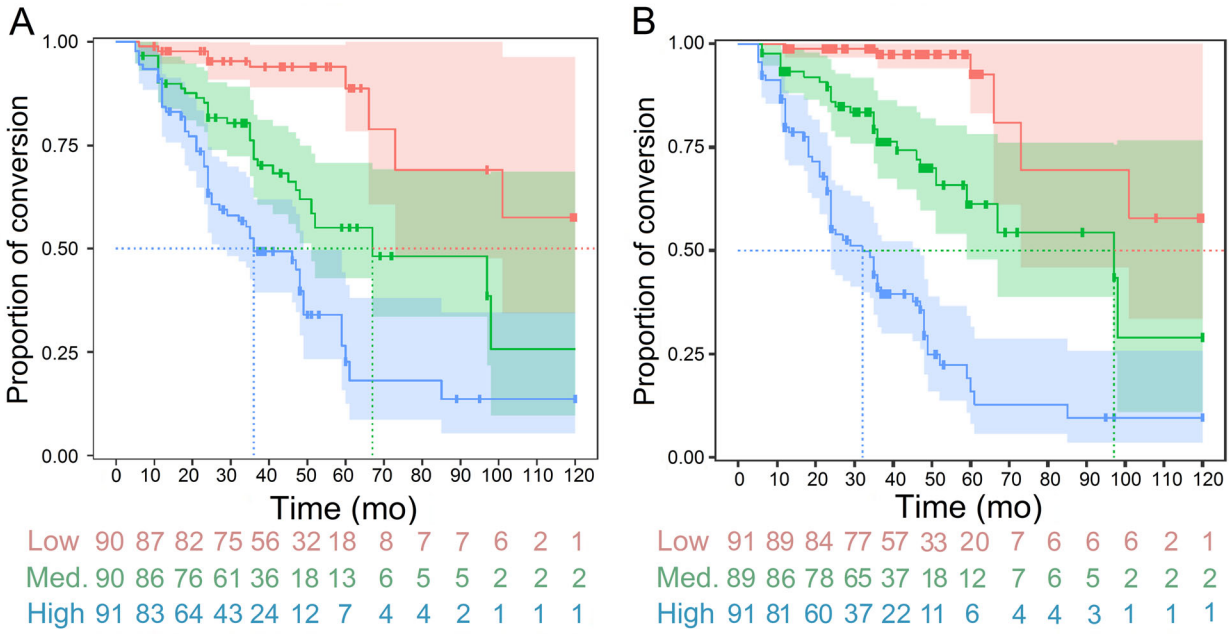

FIGURE 3. **Kaplan-Meier curves of the test dataset**. A – risk strata using the PES alone, B – risk strata using the PI of the combined model. PES, pattern expression score; PI, prognostic index.

TABLE 1. Clinical and demographic characteristics of the training and test datasets.

	Training dataset (n = 272)		**Test dataset (n = 272)**	
	MCI-c (n = 87)	**MCI-nc (n = 185)**	**MCI-c (n = 94)**	**MCI-nc (n = 178)**
Age [years]	75 ± 7	74 ± 8	73 ± 7	73 ± 8
Sex [M/F]	56/31	116/69	54/40	108/70
MMSE	27 ± 2	28 ± 2	27 ± 2	28 ± 2
APOE ε4 positive rate	63%	43%	70%	42%
FAQ	1.74 ± 3.1	4.44 ± 4.7	1.70 ± 3.0	4.97 ± 4.7
Median follow-up time, [95%CI] and (interquartile range) [months]	48 [47-49] (21.3)	47 [47-49] (26.5)	47 [46-48] (29.0)	47 [46-48] (18.0)

TABLE 2. Characteristics of the Cox regression models.

Model	Predictor	Hazard ratio	P-value	AIC	Harrell's C Training dataset	Harrell's C Test dataset
Imaging model	PES	2.96	2×10^{-16}	783.3[b,c]	0.76	0.73
	Age	1.01	0.87			
	Sex	0.98	0.93			
Clinical model	Age	1.00	0.95	797.2[a,c]	0.80	0.77
	Sex	1.18	0.48			
	FAQ	1.66	2.0×10^{-10}			
	APOE	1.85	0.007			
	MMSE	1.54	3.5×10^{-5}			
Combined model	PES	2.46	7.1×10^{-13}	749.6[a,b]	0.84	0.81
	Age	1.01	0.90			
	Sex	1.08	0.72			
	FAQ	1.49	2.2×10^{-6}			
	APOE	1.36	0.18			
	MMSE	1.51	0.0001			

All continuous variables are z-transformed. Significance level: [a] $p = 8\times10^{-9}$, [b] $p = 4\times10^{-10}$, [c] $p = 0.007$. AIC, Akaike information criterion.

TABLE 3. Separation of risk strata by different models.

	Hazard ratio			Median time to conversion (months)			Pairwise Log-Rank P-value		
	Low risk	Medium risk	High risk	Low risk	Medium risk	High risk	Low vs Medium	Medium vs High	Low vs High
PES alone	1	4.62	9.70	120	68	36	1.2×10^{-5}	0.0007	3.0×10^{-13}
PI of Combined model	1	4.75	15.92	120	96	32	8.3×10^{-8}	1.2×10^{-5}	2.0×10^{-16}

Supplementary Figure 1

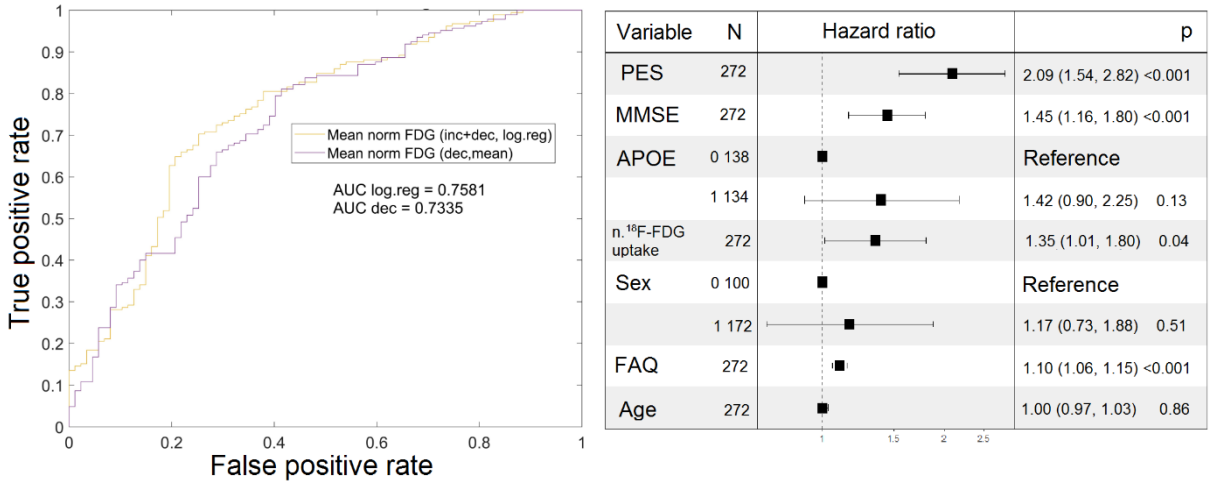

Supplementary Table 1. Characteristics of the Cox regression models (SPM).

Model	Predictor	Hazard ratio	P-value	AIC	Harrell's C Training dataset	Harrell's C Test dataset
Imaging model						
	Norm. FDG uptake	2.89	2×10^{-16}	788.7[b,c]	0.76	0.73
	Age	1.06	0.57			
	Sex	1.08	0.73			
Clinical model						
	Age	1.00	0.95	797.2[a, c]	0.80	0.77
	Sex	1.18	0.48			
	FAQ	1.66	2.0×10^{-10}			
	APOE	1.85	0.007			
	MMSE	1.54	3.5×10^{-5}			
Combined model						
	Norm. FDG uptake	2.44	7.5×10^{-12}	751.6[a, b]	0.84	0.81
	Age	1.04	0.68			
	Sex	1.16	0.52			
	FAQ	1.63	1.2×10^{-8}			
	APOE	1.61	0.03			
	MMSE	1.37	0.002			

All continuous variables are z-transformed. Significance level: [a] $p = 5\times10^{-12}$, [b] $p = 2\times10^{-9}$, [c] $p = 0.1$. FDG uptake stems from the linear combination of hypo- and hypermetabolic VOIs. AIC, Akaike information criterion.

The Journal of NUCLEAR MEDICINE

Principal component analysis of brain metabolism predicts development of Alzheimer's dementia

Ganna Blazhenets, Yilong Ma, Arnd Sörensen, Gerta Rücker, Florian Schiller, David Eidelberg, Lars Frings and Philipp T Meyer

J Nucl Med.
Published online: November 2, 2018.
Doi: 10.2967/jnumed.118.219097

The Journal of Nuclear Medicine is published monthly.
SNMMI | Society of Nuclear Medicine and Molecular Imaging
1850 Samuel Morse Drive, Reston, VA 20190.
(Print ISSN: 0161-5505, Online ISSN: 2159-662X)

SNMMI SOCIETY OF NUCLEAR MEDICINE AND MOLECULAR IMAGING